



HAL
open science

Modular multilevel converter passivity-based PI control suited for balanced and unbalanced grid conditions

Gilbert Bergna, Matteo Pirro, Erik Berne, Amir Arzandé, Marta Molinas Cabrera, Roméo Ortega

► To cite this version:

Gilbert Bergna, Matteo Pirro, Erik Berne, Amir Arzandé, Marta Molinas Cabrera, et al.. Modular multilevel converter passivity-based PI control suited for balanced and unbalanced grid conditions. 2015 IEEE International Conference on Industrial Technology (ICIT), Mar 2015, Séville, Spain. pp.3072-3078, 10.1109/ICIT.2015.7125552 . hal-01262126

HAL Id: hal-01262126

<https://centralesupelec.hal.science/hal-01262126>

Submitted on 21 Jun 2022

HAL is a multi-disciplinary open access archive for the deposit and dissemination of scientific research documents, whether they are published or not. The documents may come from teaching and research institutions in France or abroad, or from public or private research centers.

L'archive ouverte pluridisciplinaire **HAL**, est destinée au dépôt et à la diffusion de documents scientifiques de niveau recherche, publiés ou non, émanant des établissements d'enseignement et de recherche français ou étrangers, des laboratoires publics ou privés.



Distributed under a Creative Commons Attribution - NonCommercial 4.0 International License

Modular Multilevel Converter Passivity-Based PI Control suited for Balanced and Unbalanced Grid Conditions

Gilbert Bergna^{*§}, *Member, IEEE*, Matteo Pirro[†], Erik Berne[‡],
Amir Arzandé^{*}, Marta Molinas Cabrera[§], *Member, IEEE* and Romeo Ortega[¶], *Fellow'99, IEEE*

^{*}Energy Department, Supélec, 91190 Gif-sur-Yvette, France

Email: gilbert.bergnadiaz@supelec.fr

[†]Dipartimento Ingegneria dell'Informazione, Università Politecnica delle Marche, 60121 Ancona, Italia

[‡]Electricité de France R&D, 77250 Moret-sur-Loing, France

Email: erik.berne@edf.fr

[¶]Laboratoire de Signaux et Systèmes, Supélec, 91190 Gif-sur-Yvette, France

[§]Norwegian University of Science and Technology, 7491 Trondheim, Norway

Email: marta.molinas@elkraft.ntnu.no

Abstract—MMC Passivity-based PI Controller: A novel non-linear global tracking controller was proposed by extending the regulation case. It consists in a linear PI that regulates two constructed signals with respect to which the incremental model of the MMC becomes passive. Estimation of x_* : A closed-loop estimator was proposed to estimate the MMC variables in steady state needed as input for the non-linear controller. Such estimator consists on a virtual MMC energy model and both of the differential current reference equations that yielded from mathematical optimization using Lagrange multipliers.

I. INTRODUCTION

Voltage Source Converter (VSC)-based High Voltage Direct Current (HVDC) links [1], are currently the key technological solution for bulk power transmission over long distances. Moreover, multi-terminal HVDC connections have the potential of shifting Europe's power generation, from conventional to renewable energy sources. Such *SuperGrid* will serve as a transcontinental highway for renewable energy [2], allowing the geographical smoothing effects minimize the disadvantages inherent to the intermittent nature of renewable generation. The Modular Multilevel Converter introduced in [3] will be the power electronic converter suited for such task [2], presenting several advantages with respect to its predecessors such as its high modularity, scalability and lower losses, although bringing challenging control and stabilization issues that must be addressed.

There has been a clear tendency of controlling the modular multilevel converter (MMC) in its natural “abc” reference frame, instead of the commonly used “dqo” or “ $\alpha\beta o$ ” frame that results from applying the well known Park or Clarke transformations. This interest arises in order to be able to regulate in a simple and direct way the energy stored in each phase of the MMC, unlike the three-level VSC that presents only solid state switches unable to store energy. The control strategy proposed in [4] has proven to be robust thanks to its closed-loop nature and its independence to the system parameters, as well as it has presented a good dynamic performance. Yet, such

strategy is based on linear controllers, and since the system is highly non-linear, makes it impossible to ensure its stability.

Global asymptotic stability issues have been investigated by means of Lyapunov's proof in [5], [6]. Indeed, asymptotic stability of the MMC under open loop and closed loop control was proven, yet the validity of such proof only holds for the system under study. This means that even if global asymptotic stability was proven for two different MMC converters, the stability of the interconnection between these two systems is not ensured, and to prove it using Lyapunov's stability criteria one must consider the new and more complex system as a whole. Clearly, since we are aiming at a multi-terminal HVDC systems which are supposed to grow “organically” in Europe, the final state of such *SuperGrid* is unknown since it will be continuously expanding. With the complete picture in mind, it seems almost impossible, or at least of a great degree of complexity to ensure global asymptotic stability of the ever growing multi-source *SuperGrid* using a global approach. Therefore a modular control approach for ensuring stability of the global interconnected system is needed. Last but not least, the required technique must be simple to implement regardless of the complexity of the proof.

Passivity is a characterization of the system behavior based on energy, and it can be used to assess the stability of a single system [7]. Most importantly, the negative feedback combination of two passive systems results in a passive and stable interconnection [8], [9]. Therefore, the idea of making complex multi-terminal MMC-HVDC systems based on local passivity controllers as a modular approach for ensuring global asymptotic stability of the global and much larger system as a whole may be considered as the philosophical contribution of this article.

Moreover, it is possible to use a PI controller to render the system globally asymptotically stable via passivity, simplifying the implementation as was done in [10]–[13]. Such controllers are known to be simple, robust and widely accepted by practitioners. However, the aforementioned work requires that

the desired state variables in steady state that become the references values (x_*) of the system should be constant values, in order to solve this *regulation* problem. As mentioned earlier, the aim is to control the MMC in the “abc” frame which implies that the reference state variables of the system, that is to say, the differential and grid currents (i_{diff*} and i_{v*}), and the upper and lower capacitor arm voltages sum (u_{cu*}^Σ and u_{cl*}^Σ) are not constants, turning the *regulation* problem of [10]–[13] into a *tracking* problem instead.

Hence the extension of the passivity-based PI controller of [10]–[13] from the *regulation* case to the *tracking* scenario is applied to the MMC as one of the main contributions of this work. However, the success of the implementation of this new control strategy strongly depends on the estimation of the steady state signals x_* that are to be tracked. Such crucial issue is thoroughly discussed in this article, and a closed loop estimator using a virtual energy model of the MMC along with two different differential current control references that yielded from an analytical optimization problem based on Lagrange multipliers [4], [14] is proposed, capable of controlling the MMC in a phase-independent fashion or for preventing power oscillations caused in the unbalanced AC grid to flow to the DC side of the MMC.

The remainder of this article is organized as follows. The passivity-based PI controller is presented in section II. In order to successfully apply the control strategy, one must be able to estimate the steady state trajectories of the MMC variables. In IV is discussed how to calculate these tracking references for phase independent control and for constant DC power during unbalanced grid conditions. Simulations results are performed and their results are given in Section V. Finally, conclusions in Section VI complete the brief.

II. CONTROL THEORY

A. Global Tracking Problem

Consider the bilinear system

$$\dot{x}(t) = Ax(t) + d(t) + \sum_{i=1}^m u_i(t)B_i x(t) \quad (1)$$

where¹ $x, d \in \mathbb{R}^n$ are the state and the (measurable) disturbance vector, respectively, $u \in \mathbb{R}^m$, $m \leq n$, is the control vector, and $A, B_i \in \mathbb{R}^{n \times n}$ are real constant matrices.

Given an admissible, differentiable trajectory, that is a function $x_* : \mathbb{R}_+ \rightarrow \mathbb{R}^n$ verifying

$$\dot{x}_* = Ax_* + d + \sum_{i=1}^m u_i^* B_i x_* \quad (2)$$

for some control signal $u_* : \mathbb{R}_+ \rightarrow \mathbb{R}^m$. Find, if possible, a dynamic state–feedback controller of the form

$$\dot{z} = F(x, x_*) \quad (3)$$

$$u = H(x, x_*), \quad (4)$$

where $F : \mathbb{R}^n \times \mathbb{R}^n \rightarrow \mathbb{R}^q$, $q \in \mathbb{Z}_+$, and $H : \mathbb{R}^n \times \mathbb{R}^n \rightarrow \mathbb{R}^m$, such that all signals remain bounded and

$$\lim_{t \rightarrow \infty} [x(t) - x_*(t)] = 0, \quad (5)$$

for all initial conditions $(x(0), z(0)) \in \mathbb{R}^n \times \mathbb{R}^q$.

In this paper we characterize a set of matrices $\{A, B_i\}$ for which it is possible to solve the aforementioned global tracking problem with a simple *linear PI controller*. The class is identified via the following LMI.

Assumption 1: $\exists P \in \mathbb{R}^{n \times n}$, $P = P^\top > 0$ such that

$$\text{sym}(PA) \leq 0 \quad (6)$$

$$\text{sym}(PB_i) = 0, \quad (7)$$

where $\text{sym} : \mathbb{R}^{n \times n} \rightarrow \mathbb{R}^{n \times n}$ computes the symmetric part of the matrix.

To simplify the notation in the sequel we define the positive semidefinite matrix

$$Q := -\text{sym}(PA). \quad (8)$$

B. Passivity of the Bilinear Incremental Model

Lemma 1: Consider the system (1) verifying the LMI of Assumption 1 and an admissible trajectory x_* . Define the incremental signals

$$\tilde{(\cdot)} := (\cdot) - (\cdot)_*,$$

and the output function

$$y := C(x_*)x \quad (9)$$

where the map $C : \mathbb{R}^n \rightarrow \mathbb{R}^{m \times n}$ is defined as

$$C := \begin{bmatrix} x_*^\top B_1^\top \\ \vdots \\ x_*^\top B_m^\top \end{bmatrix} P.$$

The operator $\tilde{u} \mapsto y$ is passive with storage function

$$V(\tilde{x}) := \frac{1}{2} \tilde{x}^\top P \tilde{x}. \quad (10)$$

Thus, the system verifies the dissipation inequality

$$\dot{V} \leq \tilde{u}^\top y.$$

C. A PI Global Tracking Controller

From Lemma 1 the next corollary follows immediately.

Corollary 1: Consider the system (1) verifying the LMI of Assumption 1 and an admissible trajectory x_* in closed loop with the PI controller

$$\begin{aligned} \dot{z} &= -y \\ u &= -K_p y + K_i z + u_* \end{aligned} \quad (11)$$

with output (9) and $K_p = K_p^\top > 0$, $K_i = K_i^\top > 0$. For all initial conditions $(x(0), z(0)) \in \mathbb{R}^n \times \mathbb{R}^m$ the trajectories of the closed-loop system are bounded and

$$\lim_{t \rightarrow \infty} y_a(t) = 0, \quad (12)$$

where the augmented output $y_a : \mathbb{R}_+ \rightarrow \mathbb{R}^{m+n}$ is defined as

$$y_a := \begin{bmatrix} C \\ Q \end{bmatrix} \tilde{x}.$$

¹For brevity, in the sequel the time argument is omitted from all signals.

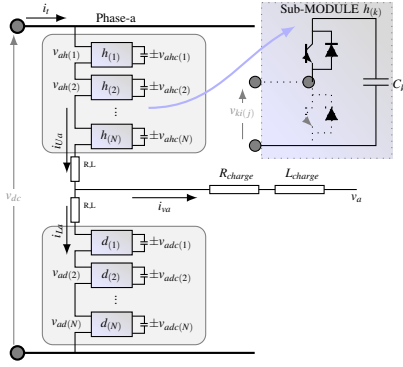


Figure 1. a) One-leg topology of a modular multilevel converter

Moreover if

$$\text{rank} \begin{bmatrix} C \\ Q \end{bmatrix} \geq n, \quad (13)$$

then global tracking is achieved, *i.e.*, (5) holds.

Remark 1: Notice that the matrix C depends on the reference trajectory. Therefore, the rank condition (13) identifies a class of trajectories for which global tracking is ensured.

Remark 2: Condition (13) is sufficient, but not necessary for state convergence. Indeed, as shown in [15], global tracking is guaranteed if y_a is a detectable output for the closed-loop system. That is, if the following implication holds

$$y_a(t) \equiv 0 \implies \lim_{t \rightarrow \infty} [x(t) - x_*(t)] = 0.$$

III. MMC APPLICATION

The model of the MMC converter (fig. 1) is

$$\begin{aligned} \dot{i}_{diff} &= -\frac{R}{L} i_{diff} - \frac{1}{4L} u_{C\Sigma} u_{\Sigma} - \frac{1}{4L} u_{C\Delta} u_{\Delta} + \frac{V_{dc}}{2L} \\ \dot{i}_v &= -\frac{R'}{L'} i_v - \frac{1}{4L'} u_{C\Delta} u_{\Sigma} - \frac{1}{4L'} u_{C\Sigma} u_{\Delta} - \frac{V_{pcc}}{L'} \\ \dot{u}_{C\Sigma} &= \frac{1}{C'} i_{diff} u_{\Sigma} + \frac{1}{2C'} i_v u_{\Delta} \\ \dot{u}_{C\Delta} &= \frac{1}{2C'} i_v u_{\Sigma} + \frac{1}{C'} i_{diff} u_{\Delta} \end{aligned} \quad (14)$$

Four state variables are considered: 1) The differential or circulating current of the MMC i_{diff} , 2) the grid or load current i_v , 3) the sum between the upper and lower capacitor voltages $u_{C\Sigma} = u_{CU} + u_{CL} = u_C^{\Sigma}$, and 4) the difference between them $u_{C\Delta} = u_{CU} - u_{CL} = u_C^{\Delta}$.

Then, using the notation of (1) we define

$$\begin{aligned} A &= \begin{bmatrix} -\frac{R}{L} & 0 & 0 & 0 \\ 0 & -\frac{R'}{L'} & 0 & 0 \\ 0 & 0 & 0 & 0 \\ 0 & 0 & 0 & 0 \end{bmatrix}, d = \begin{bmatrix} \frac{V_{dc}}{2L} \\ -\frac{V_{pcc}}{L'} \\ 0 \\ 0 \end{bmatrix} \\ B_{\Sigma} &= \begin{bmatrix} 0 & 0 & \frac{-1}{4L} & 0 \\ 0 & 0 & 0 & \frac{-1}{4L'} \\ \frac{1}{C'} & 0 & 0 & 0 \\ 0 & \frac{1}{2C'} & 0 & 0 \end{bmatrix}, B_{\Delta} = \begin{bmatrix} 0 & 0 & 0 & \frac{-1}{4L} \\ 0 & 0 & \frac{-1}{4L'} & 0 \\ 0 & \frac{1}{2C'} & 0 & 0 \\ \frac{1}{C'} & 0 & 0 & 0 \end{bmatrix}, \end{aligned}$$

and the matrix P of assumption (1) is

$$P = \begin{bmatrix} 2L & 0 & 0 & 0 \\ 0 & L' & 0 & 0 \\ 0 & 0 & \frac{C'}{2} & 0 \\ 0 & 0 & 0 & \frac{C'}{2} \end{bmatrix}.$$

It follows that, defining $x^{\top} := [i_{diff} \quad i_v \quad u_{C\Sigma} \quad u_{C\Delta}]^{\top}$, the passive output of the system is

$$\begin{aligned} y_{MC} &= \begin{bmatrix} x_{\star}^{\top} B_{\Sigma}^{\top} \\ x_{\star}^{\top} B_{\Delta}^{\top} \end{bmatrix} P x \\ &= \frac{1}{2} \begin{bmatrix} i_{diff\star} u_{C\Sigma} - i_{diff} u_{C\Sigma\star} + \frac{1}{2} i_{v\star} u_{C\Delta} - \frac{1}{2} i_v u_{C\Delta\star} \\ i_{diff\star} u_{C\Delta} - i_{diff} u_{C\Delta\star} + \frac{1}{2} i_{v\star} u_{C\Sigma} - \frac{1}{2} i_v u_{C\Sigma\star} \end{bmatrix}. \end{aligned} \quad (15)$$

Detectability is given by the rank of the matrix

$$\begin{bmatrix} C \\ Q \end{bmatrix} = \begin{bmatrix} -u_{C\Sigma\star} & -\frac{1}{2} u_{C\Delta\star} & i_{diff\star} & \frac{1}{2} u_{C\Delta\star} \\ -u_{C\Delta\star} & -\frac{1}{2} u_{C\Sigma\star} & \frac{1}{2} i_{v\star} & i_{diff\star} \\ 2R & 0 & 0 & 0 \\ 0 & R' & 0 & 0 \\ 0 & 0 & 0 & 0 \\ 0 & 0 & 0 & 0 \end{bmatrix}$$

which satisfies condition (13) whenever $i_{diff\star}^2 - \frac{1}{4} i_{v\star} u_{C\Delta\star} \neq 0$ which is satisfied in practice.

IV. REFERENCES CALCULATION

A. Generation of references in an Open Loop fashion for Phase-Independent Control

The grid current reference equilibrium point is imposed based on the desired voltage reference of the load. For the system under study with no grid connection (*i.e.*, $V_{pcc} = 0$) such reference is expressed as follows:

$$i_{v\star} = \frac{|e_{v\star}|}{\sqrt{R'^2 + (\omega L')^2}} \sin\left(\omega t - \tan^{-1}\left(\frac{\omega L'}{R'}\right)\right) \quad (16)$$

Where $e_{v\star}$ is the sinusoidal voltage that one wishes to apply to the load, with an amplitude that can vary from 0 to $\frac{V_{dc}}{2}$. In addition, $R' = \frac{R}{2} + R_{load}$ and $L' = \frac{L}{2} + L_{load}$. The differential or circulating current reference $i_{diff\star}$ is estimated by assuming a small internal resistance R :

$$i_{diff\star} \approx \frac{|e_{v\star} i_{v\star}|}{V_{dc}} \quad (17)$$

Since $i_{diff\star}$ is constant (for this case), the voltage that drives it may be expressed simply by $u_{diff\star} = R i_{diff\star}$.

Also, it is possible to calculate the fluctuations of the sum $w_{\Sigma\star}$ and difference $w_{\Delta\star}$ of the capacitive energy stored between the upper and lower arms of the MMC (see [16] for more details on such equations). Thus,

$$\begin{aligned} \Delta w_{\Sigma\star} &= \int_0^t (-e_{v\star} i_{v\star} + (V_{dc} - 2u_{diff\star}) i_{diff\star}) dt \\ \Delta w_{\Delta\star} &= \int_0^t \left(\frac{i_{v\star}}{2} (V_{dc} - 2u_{diff\star}) - 2e_{v\star} i_{diff\star} \right) dt \end{aligned} \quad (18)$$

Remark 3: A high-pass filter is needed for the term that is being integrated in equation (18) to leave out the power error caused by neglecting R in equation (17).

Figure 2. Closed loop estimator for phase independent control

The average value of w_{Σ^*} and w_{Δ^*} is given as a reference from the user; typically, $W_{\Sigma\phi^*} = \frac{C}{N} V_{dc}^2$, and $W_{\Delta\phi^*} = 0$. Using the energy estimation, it is now possible to calculate the upper and lower arm voltages.

$$\begin{aligned} u_{CU^*} &= \sqrt{\frac{N}{C} [(W_{\Sigma\phi^*} + \Delta w_{\Sigma^*}) + (W_{\Delta\phi^*} + \Delta w_{\Delta^*})]} \\ u_{CL^*} &= \sqrt{\frac{N}{C} [(W_{\Sigma\phi^*} + \Delta w_{\Sigma^*}) - (W_{\Delta\phi^*} + \Delta w_{\Delta^*})]} \end{aligned} \quad (19)$$

The remaining state variables u_{Σ^*} and u_{Δ^*} may now be calculated as

$$\begin{aligned} u_{C\Sigma^*} &= u_{CU^*} + u_{CL^*} \\ u_{C\Delta^*} &= u_{CU^*} - u_{CL^*} \end{aligned} \quad (20)$$

In addition, the upper and lower insertion indexes are calculated by

$$\begin{aligned} n_{u^*} &= \frac{\frac{V_{dc}}{2} - e_{v^*} - u_{diff^*}}{u_{cu^*}} \\ n_{l^*} &= \frac{\frac{V_{dc}}{2} + e_{v^*} - u_{diff^*}}{u_{cl^*}} \end{aligned} \quad (21)$$

The control at the equilibrium point is therefore defined as

$$\begin{aligned} u_{\Sigma^*} &= n_{u^*} + n_{l^*} \\ u_{\Delta^*} &= n_{uk^*} - n_{l^*} \end{aligned} \quad (22)$$

This estimation technique has been implemented successfully along with the so-called *open loop control* strategy in [5], [17]. Nonetheless, its effectiveness relies on the approximation made in (17) where the power dissipated in the internal resistance of the MMC is neglected. For high values of R , this assumption does not hold any more [6], and the estimating technique will no longer be useful. A solution for this case is proposed in the following sections.

B. Generation of references with a closed loop estimator

If the converter has a non-negligible internal resistance $R > 0$, a mismatch between the average values of powers $\overline{e_{vk}i_{vk}}$ and $\overline{v_{dc}i_{diffk}}$ will take place, making approximation (17) no longer valid. To overcome this issue, a *closed loop estimator* is proposed to calculate x_* and u_* , and is depicted in Fig. 2. The estimation technique is based on the application of equation (23):

$$i_{diff^*} = \frac{\overline{P_{\Sigma k}^{ref}} + (1 - \alpha)\overline{P_{vk}}}{v_{dc}^2} v_{dc} + \frac{\alpha P_{vk}}{v_{dc}} + \frac{-\overline{P_{\Delta k}^{ref}}}{2v_{dc}^2 (e_{vk,p.u.}^{rms})^2} e_{vk} \quad (23)$$

Equation (23) calculates the reference of the differential current of the MMC. Such equation contains two PI controllers represented by the terms $\overline{P_{\Sigma k}^{ref}}$ and $\overline{P_{\Delta k}^{ref}}$ that regulate the average values of the capacitive energy sum and difference stored in the arm of the converter ($\overline{w_{\Sigma k}}$ and $\overline{w_{\Delta k}}$). In the case the MMC would have a non-negligible internal resistance R , the PI

controller $\overline{P_{\Sigma k}^{ref}}$ will “add” the missing power that was neglected by the previous estimation technique. The difference between the proposition of [4], [14] and what is being proposed here, is that equation (23) will be applied to a *virtual MMC* instead of the real converter; that is to say that it will not participate directly in the control of the converter, yet it will generate the references needed for the control by means of the MMC state equations. The procedure is described in the following lines.

For a passive grid ($V_{pcc} = 0$) the grid/load current is defined as in 16. If the system is connected to a three-phased active grid ($V_{pcc} \neq 0$) then the grid current reference i_{v^*} is defined by equation (24):

$$i_{v^*} = \frac{P_{ac}^{ref}}{\|\mathbf{v}_{pcc}^+\|^2 + kp \cdot \|\mathbf{v}_{pcc}^-\|^2} \cdot \left(v_{pcc}^+ + kp \cdot v_{pcc}^- \right) \quad (24)$$

Equation (24) calculates the grid current in steady state (i_{v^*}), as a function of the power reference established by the secondary control P_{ac}^{ref} , and the positive and negative voltage measurements of the point of common coupling (v_{pcc}^+ and v_{pcc}^-) from the *real* MMC, and a constant kp defined by the user.

In order to calculate the differential current reference in steady state (i_{diff^*}) equation 23 is used along with a *virtual* energy model of the MMC. Such model contains the MMC energy sum and difference dynamics (\dot{w}_{Σ} and \dot{w}_{Δ})

$$\begin{aligned} \dot{w}_{\Sigma k} &= \int_0^t (-e_{v^*k} i_{v^*k} + (V_{dc} - 2u_{diff^*k}) i_{diff^*k}) dt \\ \dot{w}_{\Delta k} &= \int_0^t \left(\frac{i_{v^*k}}{2} (V_{dc} - 2u_{diff^*k}) - 2e_{v^*k} i_{diff^*k} \right) dt \end{aligned} \quad (25)$$

$$(26)$$

with e_{v^*k} and u_{diff^*k} calculated as

$$\begin{aligned} u_{diff^*k} &= R i_{diff^*k} + L \frac{d}{dt} i_{diff^*k} \\ e_{v^*k} &= R' i_{v^*k} + L' \frac{d}{dt} i_{v^*k} + V_{pcc} \end{aligned} \quad (27)$$

The average values of the w_{Σ^*} and w_{Δ^*} are required to calculate $\overline{P_{\Sigma k}^{ref}}$ and $\overline{P_{\Delta k}^{ref}}$ expressed in (28) that are in turn needed for the calculation of i_{diff^*} by (23).

$$\begin{aligned} \overline{P_{\Sigma k}^{ref}} &= \left[kp_{\Sigma} \left(W_{\Sigma k}^{ref} - \overline{w_{\Sigma k}} \right) + ki_{\Sigma} \int \left(W_{\Sigma k}^{ref} - \overline{w_{\Sigma k}} \right) dt \right] \\ \overline{P_{\Delta k}^{ref}} &= \left[kp_{\Delta} \left(W_{\Delta k}^{ref} - \overline{w_{\Delta k}} \right) + ki_{\Delta} \int \left(W_{\Delta k}^{ref} - \overline{w_{\Delta k}} \right) dt \right] \end{aligned} \quad (28)$$

In order to so whilst obtaining good dynamic performance, the average values of w_{Σ^*} and w_{Δ^*} are calculated using:

$$\begin{aligned} \hat{w}_{\Sigma^*} &= w_{\Sigma^*} - w_{\Sigma^* \alpha} \\ \hat{w}_{\Delta^*} &= w_{\Delta^*} - w_{\Delta^* \alpha} \end{aligned} \quad (29)$$

Where $w_{\Sigma\star\alpha}$ and $w_{\Delta\star\alpha}$ are band-pass-filtered signals produced by a second order generalized integrator (SOGI) - quadrature signal generator that is acting as a Notch filter.

Furthermore, $u_{cu\star}$ and $u_{cl\star}$ are calculated via (30)

$$\begin{aligned} u_{CU\star} &= \sqrt{\frac{N}{C} [w_{\Sigma\star} + w_{\Delta\star}]} \\ u_{CL\star} &= \sqrt{\frac{N}{C} [w_{\Sigma\star} - w_{\Delta\star}]} \end{aligned} \quad (30)$$

Finally, $u_{c\Sigma}$ and $u_{c\Delta}$ are calculated as in 20. This concludes the estimation of x_\star . To obtain u_\star ; i.e., the control in steady state, equations 21 and 22 are required once more.

C. Generation of references for constant DC power under unbalanced grid conditions

Nevertheless, $i_{diff\star}$ determined by equation (23) is not able to successfully cope with unbalanced grid conditions, since it is the result of an analytical mathematical optimization that does not consider the relationship between the phases of the MMC. To be able to successfully handle unbalances, by preventing power fluctuations from the unbalanced AC side of the converter to pass its DC side, $i_{diff\star}$ is calculated using equation (31):

$$\begin{aligned} i_{diff\star k} &= \frac{\bar{P}_{\Sigma\star k}^{ref} + (1-\alpha)\bar{P}_{v\star k}}{v_{dc}^2} v_{dc} + \frac{\alpha P_{v\star k}}{v_{dc}} + \frac{-\bar{P}_{\Delta\star k}^{ref} e_{v\star k}}{2v_{dc}^2 (e_{v\star k, p.u.}^{rms})^2} \\ &\quad - \sum_{k \in (abc)} \left(\frac{\bar{P}_{\Sigma\star k}^{ref} + (1-\alpha)\bar{P}_{v\star k}}{v_{dc}^2} v_{dc} + \right. \\ &\quad \left. \frac{\alpha P_{v\star k}}{v_{dc}} + \frac{-\bar{P}_{\Delta\star k}^{ref} e_{v\star k}}{2v_{dc}^2 (e_{v\star k, p.u.}^{rms})^2} \right) + \frac{1}{3} \frac{P_{dc}^{ref}}{v_{dc}} \end{aligned} \quad (31)$$

As was done for the previous case, equation (31) must be combined with the *virtual* energy model of the MMC expressed in (26). This is since (31) requires closing the energy regulation loop with three the PI controllers represented by $\bar{P}_{\Sigma\star k}^{ref}$, $\bar{P}_{\Delta\star k}^{ref}$ and, for the direct power assignment case, P_{dc} .

1) *The Controller*: To summarize, the controller equations are:

$$\begin{aligned} \dot{z}_{MC} &= -y_{MC} \\ u_{MC} &= -K_p y_{MC} + K_i z_{MC} + [u_{\Sigma\star} \quad u_{\Delta\star}]^T \\ y_{MC} &= \frac{1}{2} \left[i_{diff\star} u_{C\Sigma\star} - i_{diff\star} u_{C\Delta\star} + \frac{1}{2} i_{v\star} u_{C\Delta} - \frac{1}{2} i_{v\star} u_{C\Sigma\star} \right] \\ &\quad - \frac{1}{2} \left[i_{diff\star} u_{C\Delta} - i_{diff\star} u_{C\Sigma\star} + \frac{1}{2} i_{v\star} u_{C\Sigma} - \frac{1}{2} i_{v\star} u_{C\Delta} \right] \end{aligned}$$

With reference variables $i_{v\star}$ defined in (24), $i_{diff\star}$ in (23) for phase independent control and in (31) for constant DC power control; $u_{C\Sigma\star}$ and $u_{C\Delta\star}$ are defined by replacing (30) in (20). In addition, $u_{\Sigma\star}$ and $u_{\Delta\star}$ are derived in (21) and (22).

V. RESULTS

To validate the proposed control, simulations have been carried out.

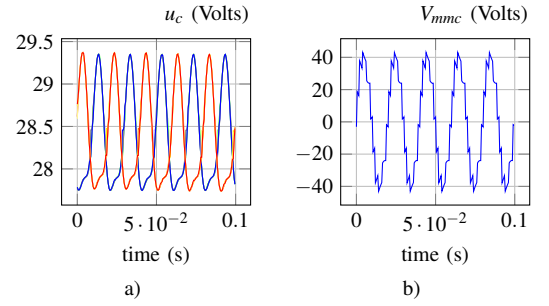


Figure 3. MMC 2N Individual Capacitor Voltages, b) MMC output voltage

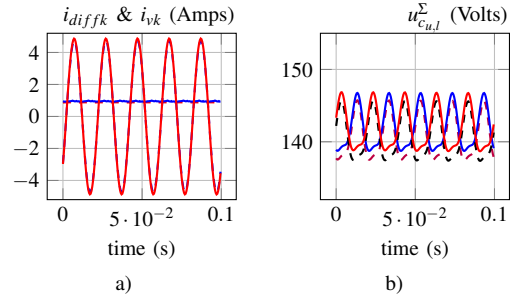


Figure 4. Phase-independent control of a single phased MMC: a) Differential and Grid Current; b) MMC Sum of capacitor voltages by arm.

A. Phase Independent Control

A single-phase MMC simulation scenario has been set up in Matlab/Simulink using a high efficiency model [18] to test the validity of the control. The considerations are the following : the converter has $2N = 10$ submodules, N in each arm (upper and lower). The input DC voltage is $V_{dc} = 140V$, the reference voltage $e_{v\star}$ has an amplitude of $\frac{V_{dc}}{2}$ and a frequency set to $f = 50Hz$. The frequency of the balancing algorithm [16] that balances the N capacitor voltages is set to $f = 20kHz$. The internal capacitance, resistance and inductance are respectively set to $C = 3.3mF$, $R = 12\Omega$ and $L = 10mH$. The load resistance and inductance values, respectively, are $R = 12\Omega$ and $L = 40mH$.

Figure 3-a) shows the $2N$ voltage trends of the MMC capacitors, whereas in 3-b) is depicted the AC output voltage multilevel waveform of the converter. Furthermore, the state references x_\star as well as the measured state variable are depicted in Fig. 4. As can be seen from Fig. 4-a) and Fig. 4-b), the i_{diff} and i_v converge to $i_{diff\star}$ and $i_{v\star}$. Nonetheless in Fig. 4-c) a non-negligible error between $u_{c_{u,l}\star}^\Sigma$ and $u_{c_{u,l}}^\Sigma$ of $\approx 1Volt$ can be observed. Fortunately, $u_{c_{u,l}}^\Sigma$ is the sum all the N capacitors in the upper or lower arm, thus the error of the individual capacitor voltage $u_{c_i} \approx 1/5Volts$. Such error occurs since there is still a remaining power mismatch, even after reducing it using the proposed closed loop estimator along with the *virtual* energy model. This occurs since the high frequency current harmonics caused by the modulation, and eventually by the saturation of the insertion indexes, are not considered in such model. These current harmonics produces losses when passing through the MMC resistances, and cause the error in the estimation.

Table I. MMC PARAMETERS

Parameter	Value
DC Voltage	150 Volts
Number of SM per arm	5
SM Nominal Voltage	30 Volts
SM Capacitance	3.3 mF
Arm Inductance	20 mH
Arm Resistance	6 Ω
Load Inductance	20 mH
Load Resistance	6 Ω

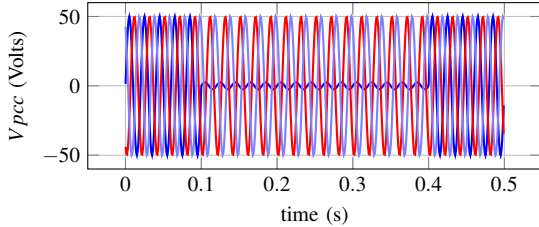


Figure 5. Voltage at the point of common coupling

B. Constant DC Power Control

In this section, a three-phased MMC converter connected to an active grid has been simulated under unbalanced conditions in order to test the proposed control along with the closed-loop estimator for constant DC power control. The simulation scenario was done by establishing the primary power reference of the system at the point of common coupling via P_{ac}^{ref} , as well as establishing it at the DC terminals of the MMC via P_{dc}^{ref} . The MMC parameters are given in table I. This series of simulation analyzes the performance of the controller when at $t = 0.1s$ the voltage at the point of common coupling of phase “a” is reduced to 5% of its original value and remains at that value for a total time of 0.3s, before returning to its original level at $t = 0.4$. This is depicted in Fig. 5.

In Fig. 6-a) are depicted the power at the point of common coupling P_{ac} in blue and the power at the DC terminals of the MMC P_{dc} in red. It can be seen that during the fault P_{ac} starts fluctuating at twice the grid frequency. Nonetheless, such oscillations are blocked by the energy storing elements of the MMC, and do not appear at the DC side of the converter. This holds independently of how the primary power reference of the system is being established. However, for the primary power reference is established at the DC terminals of the MMC, it seems that the power oscillations are most effectively decoupled as even transient perturbations have been removed. Nonetheless, this case imposes a more elevated energy and voltage stress to its capacitors as can be seen in Fig. 6-b) and 6-c), and have to be oversized to withstand this scenario.

In Fig. 6-c), 6-d) and 6-e) are shown the waveform trends of the references and the state of the system (x_* and x): the differential currents, the grid currents, and the capacitor voltages, respectively. A familiar result comes to mind: the grid and circulating currents are regulated quite well, whereas a stationary regulation error is found between reference and measurements of the capacitor voltages. The error is approximately of the order of 2%. Here again, it is caused by the power mismatch error in the estimation. Furthermore, the grid currents stay balanced in both cases since $kp = 0$ is used in (24) [19], [20].

VI. CONCLUSIONS

In this brief, a passivity-based PI controller has been applied to the modular multilevel converter in the ABC frame. Global asymptotic stability is ensured with a simple PI regulating the MMC passive outputs to zero. The obtained stability results are global and hold for all positive definite gains of the PI. The performance of the controller was tested by means of some realistic simulations for the MMC. The converter showed good performance despite the estimation error caused by neglecting the high order harmonics and physical limits including control saturation. The proposed estimation technique is capable of considering the power losses caused by the fundamental harmonics of each current in the internal resistance of the MMC, usually neglected in “open loop” approaches. Furthermore, it can be used to generate the necessary references x_* necessary for preventing power oscillations caused by an unbalanced grid from appearing at the DC terminals of the MMC. However, the estimation is model-based, which is usually a drawback during the practical implementation due to the parameters uncertainty. Last but not least, passivity offers a local approach to ensure stability of complex MMC-based multi-terminal HVDC systems

REFERENCES

- [1] N. Flourentzou, V. Agelidis, and G. Demetriades, “Vsc-based hvdc power transmission systems: An overview,” *Power Electronics, IEEE Transactions on*, vol. 24, no. 3, pp. 592–602, March 2009.
- [2] N. Ahmed, A. Haider, D. Van Hertem, L. Zhang, and H.-P. Nee, “Prospects and challenges of future hvdc supergrids with modular multilevel converters,” in *Power Electronics and Applications (EPE 2011), Proceedings of the 2011-14th European Conference on*, 30 2011-sept. 1 2011, pp. 1–10.
- [3] A. Lesnicar and R. Marquardt, “An innovative modular multilevel converter topology suitable for a wide power range,” in *Power Tech Conference Proceedings, 2003 IEEE Bologna*, vol. 3, june 2003, p. 6 pp. Vol.3.
- [4] G. Bergna, A. Garces, E. Berne, P. Egrot, A. Arzande, J.-C. Vannier, and M. Molinas, “A generalized power control approach in abc frame for modular multilevel converter hvdc links based on mathematical optimization,” *Power Delivery, IEEE Transactions on*, vol. PP, no. 99, pp. 1–9, 2013.
- [5] A. Antonopoulos, L. Angquist, L. Harnefors, K. Ilves, and H.-P. Nee, “Global asymptotic stability of modular multilevel converters,” *Industrial Electronics, IEEE Transactions on*, vol. 61, no. 2, pp. 603–612, 2014.
- [6] L. Harnefors, A. Antonopoulos, and H.-P. Nee, “Global asymptotic stability of modular multilevel converters with measurement lag and circulating-current control,” in *Power Electronics and Applications (EPE), 2013 15th European Conference on*, 2013, pp. 1–10.
- [7] R. Ortega, *Passivity-based Control of Euler-Lagrange Systems: Mechanical, Electrical and Electromechanical Applications*, ser. Communications and Control Engineering. Springer, 1998. [Online]. Available: <http://books.google.no/books?id=HeJSAAAAMAAJ>
- [8] M. McCourt and P. Antsaklis, “Stability of networked passive switched systems,” in *Decision and Control (CDC), 2010 49th IEEE Conference on*, Dec 2010, pp. 1263–1268.
- [9] S. Stramigioli, B. Maschke, and A. V. D. Schaft, “Passive output feedback and port interconnection.” 1998.
- [10] B. Jayawardhana, R. Ortega, E. Garcia-Canseco, and F. Castanos, “Passivity of nonlinear incremental systems: Application to pi stabilization of nonlinear rlc circuits,” in *Decision and Control, 2006 45th IEEE Conference on*, 2006, pp. 3808–3812.
- [11] S. R. Sanders and G. C. Verghese, “Lyapunov-based control for switched power converters,” *Power Electronics, IEEE Transactions on*, vol. 7, no. 1, pp. 17–24, 1992.

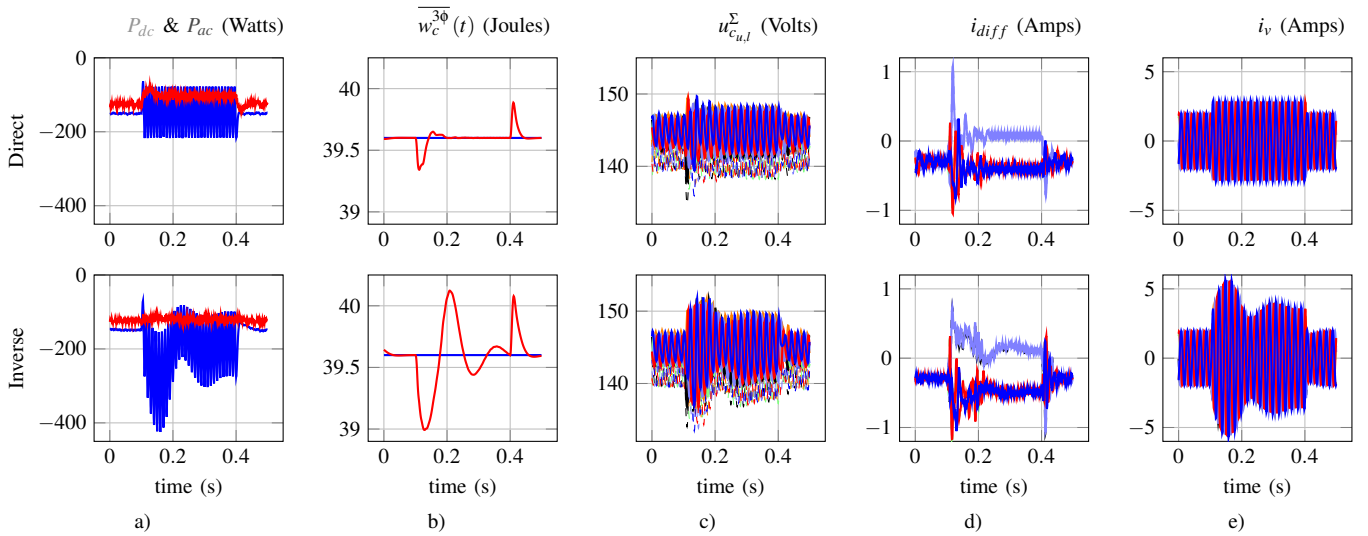


Figure 6. Power and energy trends: a) Power at the dc terminals (in red) and at the PCC (in blue), b) MMC 3-phase capacitive energy, and c) MMC individual capacitor voltages d) differential currents and e) grid currents

- [12] F. Castaños, B. Jayawardhana, R. Ortega, and E. Garca-Canseco, "Proportional plus integral control for set-point regulation of a class of nonlinear RLC circuits," *Circuits, Systems and Signal Processing*, vol. 28, no. 4, pp. 609–623, 2009.
- [13] M. Hernandez-Gomez, R. Ortega, F. Lamnabhi-Lagarrigue, and G. Escobar, "Adaptive pi stabilization of switched power converters," *Control Systems Technology, IEEE Transactions on*, vol. 18, no. 3, pp. 688–698, 2010.
- [14] G. Bergna, E. Berne, A. Garces, P. Egrot, J.-C. Vannier, and M. Molinas, "A generalized power control approach in abc frame for modular multilevel converters based on lagrange multipliers," in *Power Electronics and Applications (EPE), 2013 15th European Conference on*, 2013, pp. 1–8.
- [15] A. Van der Schaft, *L₂-Gain and passivity techniques in nonlinear control*, ser. Communications and Control Engineering Series. Springer-Verlag, 2000.
- [16] L. Harnefors, A. Antonopoulos, S. Norrga, L. Angquist, and H. Nee, "Dynamic analysis of modular multilevel converters," *Industrial Electronics, IEEE Transactions on*, vol. PP, no. 99, p. 1, 2012.
- [17] L. Angquist, A. Antonopoulos, D. Siemaszko, K. Ilves, M. Vasiladiotis, and H.-P. Nee, "Open-loop control of modular multilevel converters using estimation of stored energy," *Industry Applications, IEEE Transactions on*, vol. 47, no. 6, pp. 2516–2524, nov.-dec. 2011.
- [18] U. Gnanarathna, A. Gole, and R. Jayasinghe, "Efficient modeling of modular multilevel hvdc converters (mmc) on electromagnetic transient simulation programs," *Power Delivery, IEEE Transactions on*, vol. 26, no. 1, pp. 316–324, jan. 2011.
- [19] P. Rodriguez, A. Timbus, R. Teodorescu, M. Liserre, and F. Blaabjerg, "Flexible active power control of distributed power generation systems during grid faults," *Industrial Electronics, IEEE Transactions on*, vol. 54, no. 5, pp. 2583–2592, 2007.
- [20] F. Wang, J. Duarte, and M. Hendrix, "Pliant active and reactive power control for grid-interactive converters under unbalanced voltage dips," *Power Electronics, IEEE Transactions on*, vol. 26, no. 5, pp. 1511–